Introduction to 1D ROM of A Model Rocket Combustor

Xu, Jiayang*and Karthik Duraisamy†
University of Michigan, Ann Arbor, Michigan, 48109, U.S.A.

In this work, quasi one-dimensional projection-based reduced-order modeling (ROM) has been applied to combustion instability in a continuous variable resonance combustor (CVRC), an experiment realized and installed at Purdue University.[1]

I. Quasi-1D combustor setup

The computational domain is sketched in Fig. 1, with geometry parameters given in Table 1. To avoid discontinuity, both the step and the converging part of the nozzle are shaped using a sinusoid in this study.

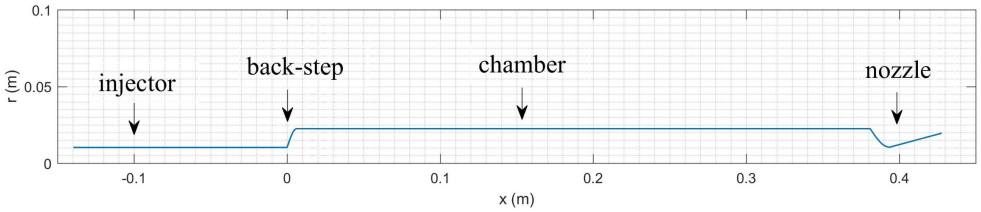

Figure 1: Computational domain

Section	Injector	Back-step	Chamber	Converging Section	Nozzle
Length (cm)	13.97	1.27	63.5	1.27	7.62
Radius (cm)	1.12	1.12 2.25	2.25	2.25 1.08	1.08 1.33

Table 1: Geometry parameters

Propellants are methane and hydrogen peroxide (more precisely 90% H_2O_2 and 10% H_2O). Operating conditions are given in Table 2.

II. Full-Order System

A. Quasi-1D Full-Order Eulerian Solver

A 1200-cell 1D grid is used for the full-order simulation. The governing equations are given in Eq. (1), which is based on previous studies[2,3] with some slight modifications.

$$\frac{\partial Q}{\partial t} + \frac{\partial F}{\partial x} = S + S_f + S_q \tag{1}$$

*Graduate Student Research Assistant, Aerospace Engineering Department, davidxu@umich.edu.
†Assistant Professor, Aerospace Engineering Department, AIAA Fellow, kdur@umich.edu.

Parameter	Value
Fuel Mass Flow Rate, kg/s	0.027
Fuel Temperature, K	300
Oxidizer Mass Flow Rate, kg/s	0.32
Oxidizer Temperature, K	1030
Mass Fraction H_2O, %	57.6
Mass Fraction O_2, %	42.4
Equivalence Ratio	0.8

Table 2: CVRC Operating conditions

where

$$Q = \begin{pmatrix} \rho \\ \rho u \\ E_0 \\ \rho Y_{ox} \end{pmatrix} \; F = \begin{pmatrix} \rho u \\ \rho u^2 + p \\ E_0 + p \\ \rho u Y_{ox} \end{pmatrix} \; S = \begin{pmatrix} 0 \\ \frac{p}{A}\frac{dA}{dx} \\ 0 \\ 0 \end{pmatrix} \; S_f = \begin{pmatrix} \dot{\omega}_f \\ \dot{\omega}_f u \\ \dot{\omega}_f \Delta h_0 \\ -\dot{\omega}_{ox} \end{pmatrix} \; S_q = \begin{pmatrix} 0 \\ 0 \\ q' \\ 0 \end{pmatrix} \tag{2}$$

The first source term, S, is due to area variations while the other two terms are related to combustion. An important assumption made here is that fuel reacts instantaneously to form products with the main consequence of neglecting intermediate species and finite reaction rates. In order to avoid discontinuities and to reproduce a combustion region of finite length, fuel is injected through a region after the back-step, between $l_s = -0.0063\ m$ and $l_f = 0.0699\ m$ with a sinusoid shape, yielding

$$\dot{\omega}_f = \frac{\dot{m}_f}{A \int (1 + \sin \xi) dx} (1 + \sin \xi) \tag{3}$$

$$\dot{\omega}_{ox} = \dot{\omega}_f / C_{f/o} \tag{4}$$

with

$$\xi = -\frac{\pi}{2} + 2\pi \frac{x - l_s}{l_f - l_s}, \text{with } l_s < x < l_f \tag{5}$$

The last contribution, S_q, refers to the unsteady heat release term. It represents the response function through which the model takes into account coupling between acoustics and combustion. Expressing the unsteady part of heat release as function of pressure with an amplification parameter α and a time lag τ.

$$q' = \dot{\omega}_f \Delta h_0 \alpha \frac{p(x, t - \tau) - \bar{p}(x)}{\bar{p}(x)} \tag{6}$$

Not being the focus of study, full-order result is briefly presented in this section to verify the solver.

B. Steady State Solutions

The steady state solution is first obtained by turning off the unsteady source term, S_q. Pressure and temperature are plotted in Fig. 2, which are identical to the result from Ref. 3.

C. Unsteady Results

In unsteady simulation, the choice of parameters are $\alpha = 3.6, \tau = T, \Delta t = 1.64 \times 10^{-7}$ s, where T is the period associated to the first longitudinal resonant frequency (1400 Hz).[2]

In order to excite pressure oscillations, a disturbance of small amplitude applied is to the mass flow rate until the pressure starts oscillating periodically. The unsteadiness is evaluated using pressure signals obtained at 36.8 cm behind the oxidizer injector. The choice of the point is related to the presence of a pressure probe at this abscissa in the experimental test.[2]

History of the pressure oscillation and its power spectral density (PSD) are presented in Fig. 3, which shows good consistency with experimental results.[1] A comparison between computed and experimental longitudinal frequencies is given in Table 3. The error is below 2%, and it should be noted that T in the model does not determine the computed value.

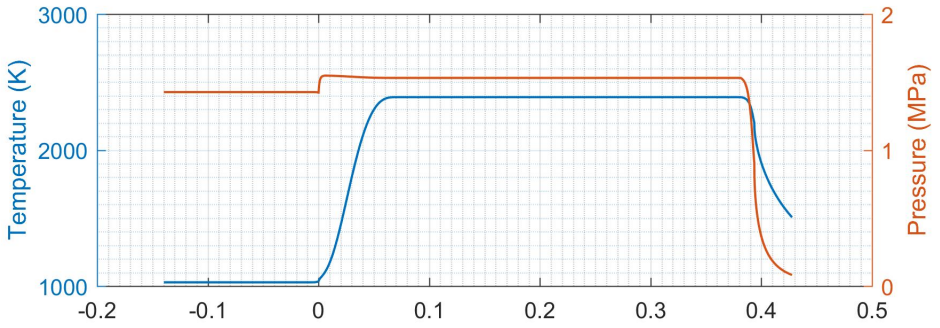

Figure 2: Steady state pressure and temperature

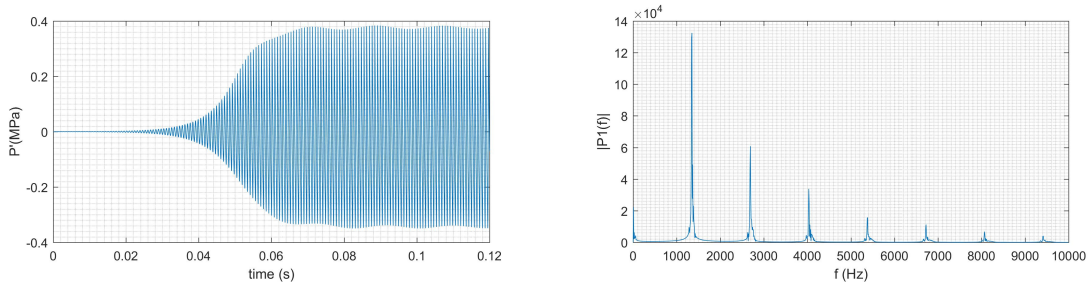

(a) Pressure oscillation history

(b) Single-sided amplitude spectrum

Figure 3: Full-order unsteady state result

III. Projection-Based Reduced-Order Modeling

A. ROM implementation

Eq. (1) can be rewritten as

$$\frac{\partial Q}{\partial t} = R\left(Q\left(x,t\right)\right) \tag{7}$$

where

$$Q = -\frac{\partial F}{\partial x} + S + S_f + S_q \tag{8}$$

At each time-step, the solution of Q at all grid points is stored in a column. Thus its dimension is $N = 4N_{elem}$.

Using full order model simulations, a snapshot matrix Q_{snap} has to be constructed, the columns of which are solutions of Q at the computed time steps. From SVD, we have $Q_{snap} = U\Sigma V^*$.

Assume M_L is the number of dimension desired to be retained, then $Q = \Phi q\left(t\right)$. Where the $N \times M_L$ matrix

$$\Phi = U_{1:M_L} \tag{9}$$

is the spatial basis matrix of Q. And q is the M_L-dimensional reduced-order variable.

Then ROM equation of Eq. (7) is

$$\frac{\partial q}{\partial t} = \Phi^T R\left(\Phi q\right) \tag{10}$$

B. Reduced-Order Modeling Results

In this study, the snapshots are taken every 100 time steps over the first 0.1 second of the FOM. Table 4 shows the number of modes needed to contain different percent of information or "energy" for each of the

Mode	1L	2L	3L
f_{exp} (Hz)	1330	2660	3990
f_{comp} (Hz)	1350	2692	4034

Table 3: Comparison between computed and experimental longitude frequencies

four variables $(\rho, \rho u, E_0, \rho Y_{ox})$, calculated from (11) for each mode.

$$\eta_i = \frac{\sigma_i}{\sum_{j=1}^{n} \sigma_j} \tag{11}$$

where σ_i is the corresponding singular value of the i-th mode. We decide to keep 151 out of 1200 modes in the ROM for each variable.

Property	90%	95%	99%
ρ	16	35	92
ρu	33	56	114
E_0	13	30	87
ρY_{ox}	14	31	82

Table 4: Modes needed for different percent of information and properties

Usually ROM is appended to the end of FOM simulations, that is, the switch from full-order to reduced-order solver in the same simulation after the last snapshot is taken. In that case, the ROM would only be working on one state where the amplitude of unsteadiness no longer changes. To test the ROM over a wider range of states, the ROM is restarted on the steady state result, following the same manner as the unsteady FOM in section C. This allows perturbations and the transition from stable to unstable states to be covered by ROM.

With more than 87% modes left out, the ROM demonstrates an ability to retain accuracy and stability with a CFL number greater than 1.

A comparison of pressure time history by ROM at different CFL numbers is given in Fig. 4(a)-4(c). In comparison, Fig. 4(d) shows the result when ROM is appended to FOM instead of restarted, with the transition point displayed in zoomed-in view (the two cycles before $t = 0.1$ s are FOM). The error in the solution is listed in Table 5, which is measured from Eq. (12). It is interesting to note that a lower CFL number does not necessarily lead to a lower error.

$$e = \frac{\|\mathcal{S}_F - \mathcal{S}_R\|_2}{\|\mathcal{S}_R\|_2} \tag{12}$$

where $\mathcal{S}_F$ and $\mathcal{S}_R$ is the full-order and reduced-order solution.

	restarted			appended
CFL	1	3	5	1
error (%)	2.16	1.60	1.88	1.19

Table 5: Error in ROM solution

C. Sparse Sampling (to be implemented)

Ideally, Eq. (10) is M_L-dimensional and thus the computing cost at each step is reduced compared with Eq. (7). However, for nonlinear problems, the calculation of the residual, R, still requires $O(N)$ evaluations). Thus we need sparse sampling to only solve for the residual at a few critical points and reconstruct the full

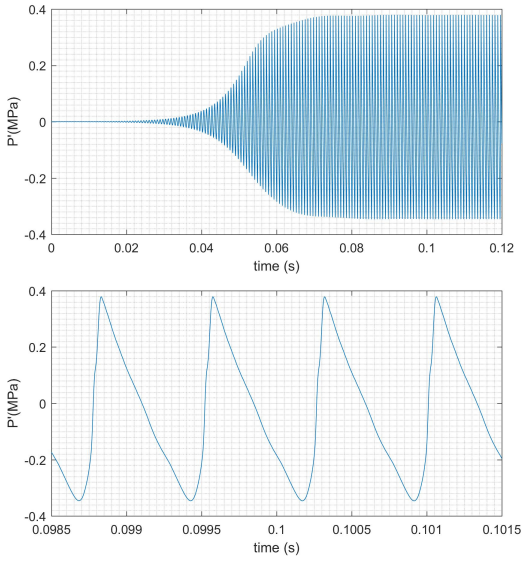

(a) CFL = 1

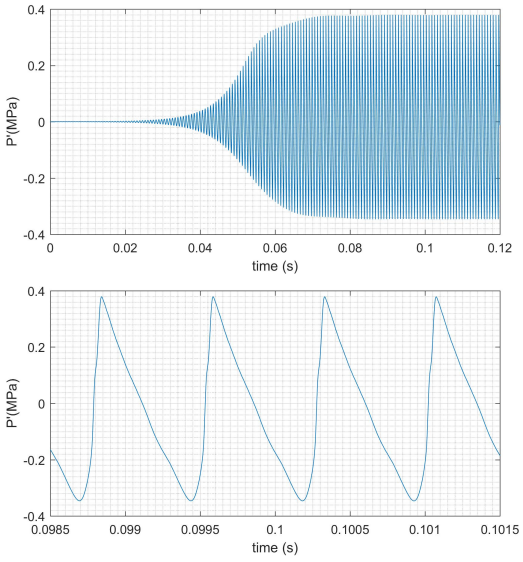

(b) CFL = 3

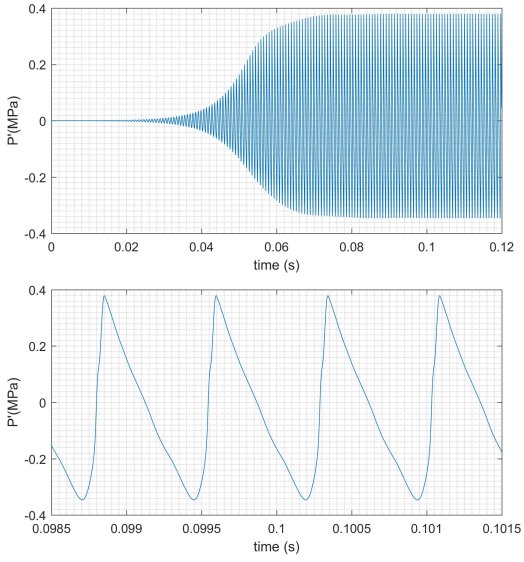

(c) CFL = 5

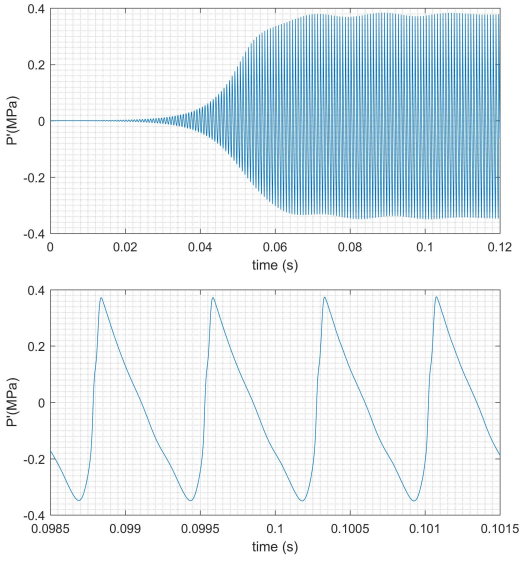

(d) FOM (0 ∼ 0.1s) + ROM (0.1 ∼ 0.12s), CFL = 1

Figure 4: Reduced-order result for pressure oscillation
(In each subfigure, top: signal history, bottom: zoomed-in view for four cycles)

residual from these solutions. We follow the discrete empirical interpolation method (DEIM)[4] for this purpose. The equations are:

$$\begin{aligned} R_{N\times 1} &= \Psi_{N\times M_L} c_{M_L\times 1} \\ \hat{R}_{M_L\times 1} &= PR = P\Psi_{N\times M_L} c_{M_L\times 1} \\ R &= \Psi \left(P\Psi\right)^{-1}_{M_L\times M_L} \hat{R} \end{aligned} \tag{13}$$

where Ψ and c are obtained using SVD on snapshots of R, in the same manner as Φ and q is obtained from Q_{snap} and

$$P = \begin{cases} 1 & \hat{x}_i = x_j \\ 0 & elsewhere \end{cases}$$

.

The critical points, $\hat{x}$, are chosen using. The DEIM procedure is given in Algorithm 1

Algorithm 1 Discrete empirical interpolation method

Input: $\Psi_{N\times M_L} = [\psi_1, \ldots, \psi_{M_L}]$
Output: $\vec{x} = [\hat{x}_1, \ldots \hat{x}_{M_L}]$
  $[\rho, \hat{x}_1] = \max\left(|\psi_1|\right)$
  $\vec{x} = [\hat{x}]$
  for $i = 2$ **to** M_L **do**
    $\psi \leftarrow \psi_i$
    Solve $\Psi_{\vec{x}} c = \psi_{\vec{x}}$ for c
    $r = \psi - \Psi c$
    $[\rho, \hat{x}_i] = \max\left(|r|\right)$
    $\vec{x} = [\vec{x}, x_i]$
  end for

To give an intuitive example, pressure distribution is reconstructed from multiple choices of M_L using DEIM and shown in Fig. 5, where the red dots are the chosen critical points.

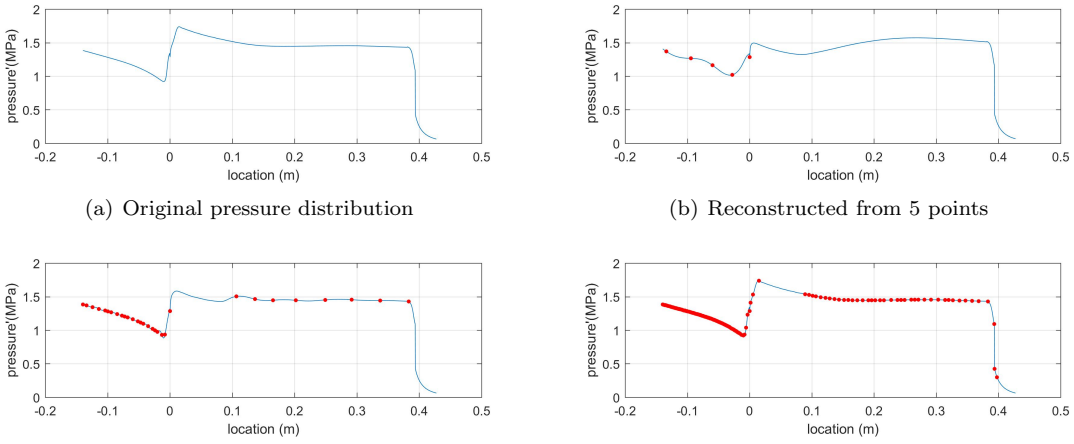

(a) Original pressure distribution

(b) Reconstructed from 5 points

(c) Reconstructed from 30 points

(d) Reconstructed from 150 points

Figure 5: DEIM reconstruction of pressure

References

[1]Harvazinski, M. E., Huang, C., Sankaran, V., Feldman, T. W., Anderson, W. E., Merkle, C. L., and Talley, D. G., "Coupling between hydrodynamics, acoustics, and heat release in a self-excited unstable combustor," *Physics of Fluids (1994-present)*, Vol. 27, No. 4, 2015, pp. 045102.

[2]Frezzotti, M. L., Nasuti, F., Huang, C., Merkle, C., and Anderson, W. E., "Response Function Modeling in the Study of Longitudinal Combustion Instability by a Quasi-1D Eulerian Solver," *51st AIAA/SAE/ASEE Joint Propulsion Conference*, 2015, p. 3840.

[3]Frezzotti, M. L., Nasuti, F., Huang, C., Merkle, C., and Anderson, W. E., "Parametric Analysis of Response Function in Modeling Combustion Instability by a Quasi-1D Solver," *6th EUROPEAN CONFERENCE FOR AEROSPACE SCIENCES*, 2015.

[4]Chaturantabut, S. and Sorensen, D. C., "Discrete empirical interpolation for nonlinear model reduction," *Decision and Control, 2009 held jointly with the 2009 28th Chinese Control Conference. CDC/CCC 2009. Proceedings of the 48th IEEE Conference on*, IEEE, 2009, pp. 4316–4321.